Title

Component and system evaluation for the development of a handheld point-of-care spatial frequency domain imaging (SFDI) device

ISBN

9780819493422

Authors

Nadeau, KP
Khoury, P
Mazhar, A
et al.

Publication Date

2013-03-13

DOI

10.1117/12.2004909

Component and system evaluation for the development of a handheld point-of-care spatial frequency domain imaging (SFDI) device

K.P. Nadeau[1], P. Khoury[2], A. Mazhar[2], D. Cuccia[2], A. J. Durkin[1]

1. Laser Microbeam and Medical Program (LAMMP), Beckman Laser Institute, 1002 Health Sciences Road, Irvine, CA 92612
2. Modulated Imaging Inc., Beckman Laser Institute Photonic Incubator, 1002 Health Sciences Road, Irvine, CA 92612

ABSTRACT

Recently, digital photography has become an efficient and economic method to assist dermatologists in monitoring skin characteristics. Although this technology has advanced a great deal in resolution and costs, conventional digital cameras continue to only provide *qualitative* recording of color information. To address this issue, we are developing a compact, *quantitative* skin imaging camera by employing spatial frequency domain imaging (SFDI), a non-contact approach for determining tissue optical properties over a wide field-of-view. SFDI uses knowledge of optical properties at multiple wavelengths to recover concentrations of tissue constituents such as oxy/deoxy-hemoglobin, water, and melanin. This method has been well researched and presented in laboratory and research settings. The next step in the development of SFDI systems is to make typical systems compact and cheaper using commercial components. We present our findings by performing a component-by-component analysis of key SFDI system components including light sources, projectors, and cameras.

KEYWORDS: near-infrared spectroscopy, spatial frequency domain imaging, modulated imaging, digital micromirror device, dermatology, quantitative functional imaging

1. INTRODUCTION

The most prominent technique to monitor tissue health in medicine remains visual inspection. The color and feel of a tissue can tell clinicians a great deal about the health of a tissue. In the same spirit, digital cameras have also become a tool to aid clinicians in monitoring various skin conditions. Cameras have become an increasingly useful tool to record tissue appearance, provide surgical guidance, and aid in assessment. Digital cameras are relatively low cost, based on advances in consumer electronics, and compact, which makes them easy to transport and store within a clinical environment.

Although digital camera technology has advanced tremendously and is pervasive in the consumer market, the data obtained is generally qualitative due to dependence on lighting conditions. Even in identical lighting conditions, a color image recorded by two similar cameras for the same object may vary significantly [1]. For certain types of skin phenomena, this camera-dependent effect on color data may change the interpretation of clinical images [2]. Varying lighting conditions can affect the appearance of an object on the same camera as well. This suggests that quantitative, objective imaging tools could have tremendous impact in clinical applications such as dermatology, which has already demonstrated a willingness to use technologies such as dermoscopy, to improve clinical assessment of suspicious tissue [3].

In recent years, a non-contact quantitative imaging technique known as spatial frequency domain imaging (SFDI) has been invented and developed at the Beckman Laser Institute. SFDI is a non-contact, wide-field imaging modality that can measure the absolute concentration of chromophores in tissue. SFDI is able to make quantitative measurements by using a well-calibrated multi-spectral light source coupled with a patterned illumination scheme and camera-based

Design and Quality for Biomedical Technologies VI, edited by Ramesh Raghavachari, Rongguang Liang, Proc. of SPIE Vol. 8573, 857304 · © 2013 SPIE
CCC code: 1605-7422/13/$18 · doi: 10.1117/12.2004909

detection. This combination of hardware allows for model based recovery of tissue optical properties. Chromophores that are typically measured in tissue include oxy/deoxy- hemoglobin, melanin, and water. SFDI has been applied to a number of skin applications including the assessment of port wine stain response to laser therapy [4], characterizing tattoo optical properties [5], assessing burn severity [6], and monitoring the health of skin flaps [7]. **Figure 1** shows a high-level illustration with the key components needed to build a basic SFDI system. These components include a projector, light source, and camera.

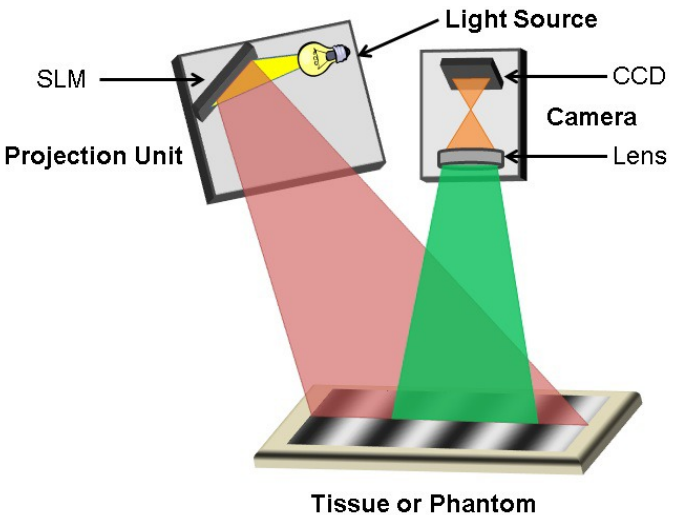

Figure 1 – Schematic of an SFDI instrument. Patterned light is impinged on a sample using a light source coupled with a spatial light modulator (SLM). The remitted light is then detected by a camera.

An extensive description and analysis of SFDI has been described by Cuccia *et al* [8]. In short, light passes through a spatial light modulator (SLM) to generate spatially modulated sinusoidal patterns, which are then projected onto the tissue. In many cases, the SLM employed is a digital micromirror device (DMD), which is commonly used in commercial projectors [8, 9]. The diffusely reflected light from the tissue enters the camera lens, and is detected by the charge-coupled device (CCD). Multiple patterns of different spatial frequencies are required to recover tissue optical properties. In order to recover the AC amplitude, we use a demodulation method first described by Neil *et al* [10]. In this embodiment, sinusoidal illumination patterns of a certain frequency are sequentially projected onto tissue with three phase shifts (0, 120, 240 degrees), and the amplitude envelope for a given spatial frequency is recovered using a demodulation term. The multiple pattern requirement makes the SLM a key component of a SFDI system.

This remitted light data is calibrated to a reference phantom with known optical properties to recover a calibrated reflectance. From the calibrated diffuse reflectance data at multiple frequencies, we can obtain the reduced scattering and absorption coefficients using Monte Carlo [9] or diffusion light transport models in the spatial frequency domain. We can then derive relevant chromophore concentrations based on the derived absorption coefficients at specific wavelengths using Beer's Law [11]. The spectral and intensity stability of the light source and camera are crucial in this calibration step as fluctuations between calibration and measurement can be misinterpreted as incorrect optical properties of the tissue sample.

Our lab has developed many generations of instrumentation. Typically, all components in our systems have been scientific grade and or in the form of developer kits with minimal focus for size and cost. Our group has also typically focused on near-infrared (NIR) illumination as it typically interrogates tissue deeper than the naked eye due to the relatively low absorption of blood and water. We feel that deeper detection is advantageous for early disease detection and we require that NIR illumination is a design requirement for new systems. Here, we propose a component evaluation as initial steps towards the development of a compact SFDI device in a similar form factor as a handheld digital camera. Our goal is to integrate the functionality of previous SFDI systems we have developed into an inexpensive, compact system tailored to clinical use for dermatology in particular.

When evaluating components for developing a handheld SFDI system, there are several considerations that are needed for each component. In this paper, we will focus primarily on grayscale linearity, light source stability, and spectral throughput. As described above, SFDI derives chromophore concentration estimates based on data taken from multiple spatial frequencies using a demodulation method. This demodulation equation assumes true sinusoidal patterns and is a requirement for any SLM. In our work with commercial projectors, we have found that this necessitates a calibration step by measuring the linear grayscale intensity output versus input curve. Also, SFDI requires data taken at specific known and stable wavelengths. Therefore, the light sources that we employ must have good spectral stability over time so that our measurements are accurate. Also, a key practical issue for any clinical measurement is artifacts due to patient motion. Although our group has developed algorithms to account for this at some level, it is still ideal to minimize our imaging times [12]. Our approach has focused on using discrete, bright sources such as light emitting diodes

(LEDS), and have reasonable spectral throughput for the desired NIR wavelengths. In order to maximize light penetration depth, the wavelengths we use are in the NIR region, and system optical throughput in this region must be considered. We will evaluate these three system properties in the context of hardware components throughout the duration of this study.

2. MATERIALS AND METHODS

2.1 Projector

As described above, the SFDI method requires illumination patterns with numerous phase shifts at multiple spatial frequencies. Therefore, we need a dynamic projection unit that can provide arbitrary patterns for our handheld device. As described previously, several current SFDI devices employ DMD-based projection units. A primary advantage of using a DMD is light throughput. For example, liquid crystal based SLMs polarize light, which significantly limits light throughput.

Our lab has typically used digital light processing (DLP) developer kits as our SLM choice. These projectors are typically expensive and have a great deal of flexibility in terms of resolution, refresh rates, and calibration. One of many potential options for cost reduction and miniaturization in a handheld projection unit is the use of commercial projectors such as the LightCrafter picoprojector (Texas Instruments Inc., Dallas, TX), which is shown in **Figure 2.**

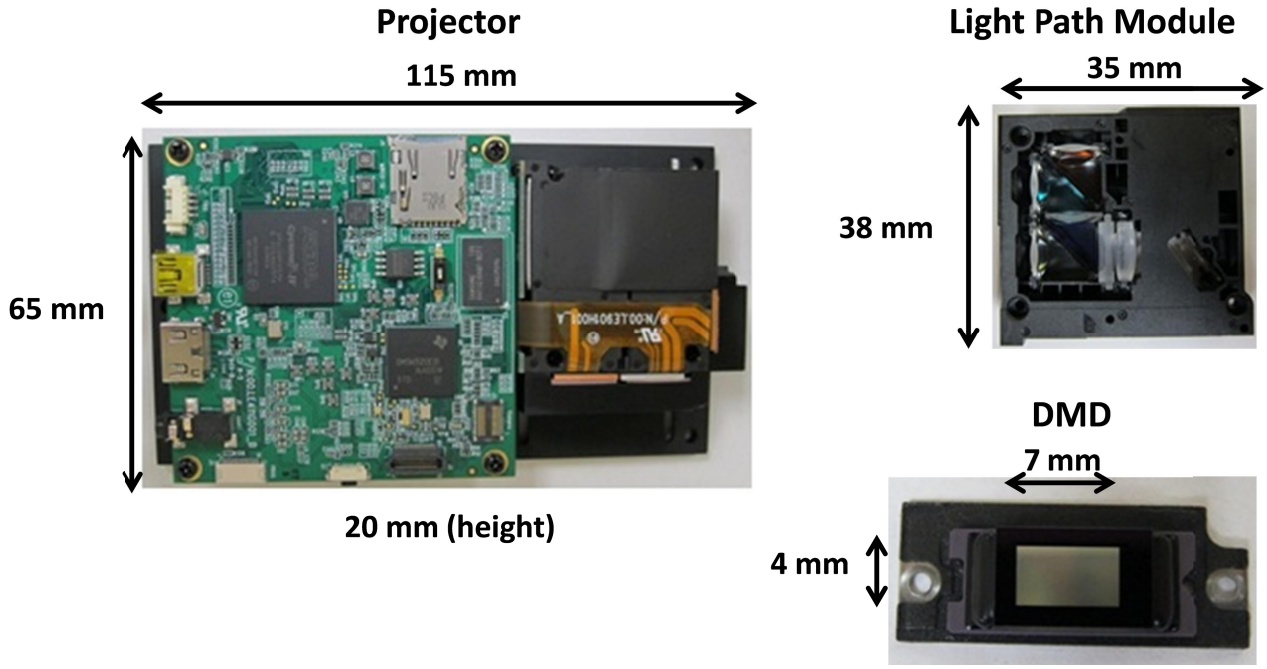

Figure 2 – Teardown of LightCrafter picoprojector, highlighting the projector (left), the light path module (top-right), and the digital micro mirror device (DMD) (bottom-right)

These commercial off the shelf projectors have several desirable properties, despite some tradeoffs with state of the art developer kits. The DMD has about the same display resolution as our state-of-the-art system (1024 x 768 mirrors vs. 684 x 608 mirrors) [4], but is more compact (14 x 10.5 mm vs. 7 x 4 mm), resulting in a higher DMD mirror density. The overall size of this unit makes it suitable to be integrated into a handheld device (115 x 65 x 20 mm). Also, the cost of the LightCrafter and other commercial projectors can be in the hundreds of dollars, which is much cheaper than units we have used in the past and are currently using. Most importantly, the form factor is compact, as shown in **Figure 2**. This component also allows for relatively straightforward connection to a personal computer for projecting custom patterns.

The first projector test that we employed was to measure the non-linearity of the system and perform a grayscale intensity calibration for projector output. Evenly distributed grayscale levels ranging from 0-255 on an 8 bit scale were projected on a 99% Spectralon reflectance standard (Labsphere Inc., North Sutton, NH) using the LightCrafter LEDs as the light source, and were detected and saved by a monochrome camera (Lumenera Corporation, model LU160m, Ottawa, ON, Canada). The pixels for each entire image obtained were averaged and used to obtain an output versus input grayscale curve. The inverse of this curve was used as our calibration curve for generating projection patterns. All data analysis and processing was done using MATLAB (Mathworks Inc., Natick, MA). This experiment was also applied to a BenQ PB8260 (BenQ Corporation, Taipei, Taiwan) projector, and an Aaxa M2 (Aaxa Technologies, Inc., Tustin, CA) projector.

The second projector test we carried out was to characterize spectral throughput of the projection unit over the visible and NIR wavelengths. In order to accomplish this, we used a broadband source as our input (OneLight Corporation, model Spectra VISNIR, Vancouver, BC, Canada). This light source produces a stable illumination over the 470-900 wavelength range. The light from this source was coupled to a fiber, which was piped through one of the LED inputs of the LightCrafter light path module. The spectrum was then read out using a OneLight Osspec handheld spectrometer (OneLight Corporation, Vancouver, BC, Canada).

2.2 Light Sources

In order to measure chromophore concentrations, we must interrogate our samples at particular wavelengths corresponding to the absorption features of our chromophores of interest (oxy/deoxy-hemoglobin, melanin, water, etc). One way of achieving this objective is to use a broadband source and employ bandpass filters to distinguish between wavelengths. Another option is to use sources with well-defined spectral peaks at desired wavelengths. The first option typically requires bulky hardware with limited optical throughput, and thus is not suitable for a handheld device. The second option presents us with components whose form factor is desirable for a handheld system. Lasers could be one option for a light source. However, they present several issues. For one, they have a very long coherence length, and are susceptible to producing speckle patterns, which are undesirable for SFDI due to spatial inhomogeneity. LEDs are a more desirable option for a handheld system. They are relatively discrete spectrally, compact, do not produce speckle patterns, and are available in a wide array of wavelengths. **Figure 3** depicts one example each of a visible and NIR LED module.

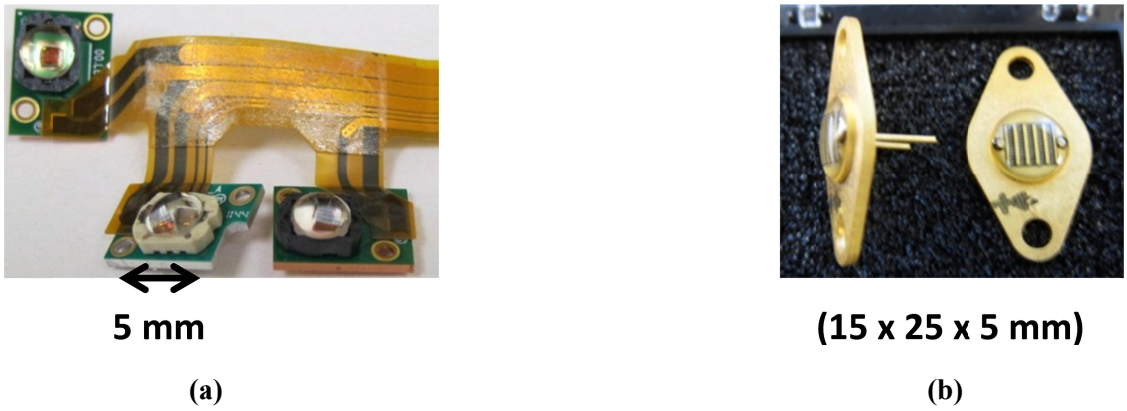

Figure 3 – Example of visible and NIR LED modules from a Texas Instruments LightCrafter (a), and a 970 nm Roithner Lasertechnik module (b)

The most important characteristics of any SFDI light source are spectral bandwidth, stability and throughput. In order to characterize these parameters, we created an experimental setup in which we placed the LED module facing a fiber with a numerical aperture of 0.22, coupled to the spectrometer entrance port. We tested a variety of LEDs including built in LEDs that were present in the LightCrafter module, and other off the shelf LEDs. LEDs from other vendors were driven by a laboratory-grade DC power supply (Agilent Technologies Inc., model E3633A, Santa Clara, CA). For the visible LightCrafter module (**Figure 3a**), we ran all LEDs at full intensity and recorded the output spectrum every five minutes for a one hour time period. We also carried this out with externally driven NIR wavelengths. We compared

the output spectrum for each LED over time to understand spectral peak shifts and overall intensity. In addition to initial spectral readings, we also investigated the effect of drive current on the spectral properties of a NIR 970 nm LED module. We did this by driving the module at seven different currents and analyzed the output spectrum. These results will be illustrated in Section 3.2.

2.3 Camera

The detection arm of SFDI consists of lenses and a CCD chip. In both cases, the spectral throughput is paramount to understanding imaging times. Here, we analyze the throughput properties of a typical consumer off-the-shelf (COTS) and research grade camera lenses, and a CCD. We decided to examine two lenses: a cheaper consumer lens commonly used in SLR cameras, as well as a higher end camera lens we have used in our current systems. These components we used are shown in **Figure 4**. The consumer and research grade lenses we analyzed were a Panasonic Lumix and Schneider Kreuznach Cinegon respectively. The experimental setup was very similar to the throughput tests described above**.** We aimed a broadband source towards the lens, and measured the output on the output end using a spectrometer.

Figure 4 – Camera components tested in this study, including a CCD detector (a), and a research (b) and COTS (c) grade lens

In order to evaluate the CCD spectral throughput, we illuminated a 99% Spectralon reflection standard with the OneLight source. We then used the customizable wavelength tunability of the OneLight System to sweep through wavelengths between 470 and 900 nm using 10 nm increments. We used the research grade lens to image the Spectralon onto the CCD. The mean of the images at each wavelength were recorded and normalized to a single wavelength (500 nm?). This was then compared to normalized spectrometer measurements of the OneLight source to determine CCD output. Both the throughput of the camera lens (measured above) and the spectrometer (previously calibrated) were accounted for in our calculation. These results, along with the lens throughput results, will be shown in Section 3.3.

3. RESULTS

3.1 Projector

In general, we have discovered that it is prudent to calibrate COTS projection units for the range of non-linear grayscale outputs. As an example, we described and performed this procedure on the LightCrafter. **Figure 5** shows grayscale output versus input curves for various COTS projection units. Although these curves varied amongst the projectors that were tested here, the non-linearity is apparent. If the non-linearity is unaccounted for, the SLM in the given projector produced inaccurate sinusoidal projections and resulted in poor demodulated image quality (**Figure 6(a)**).

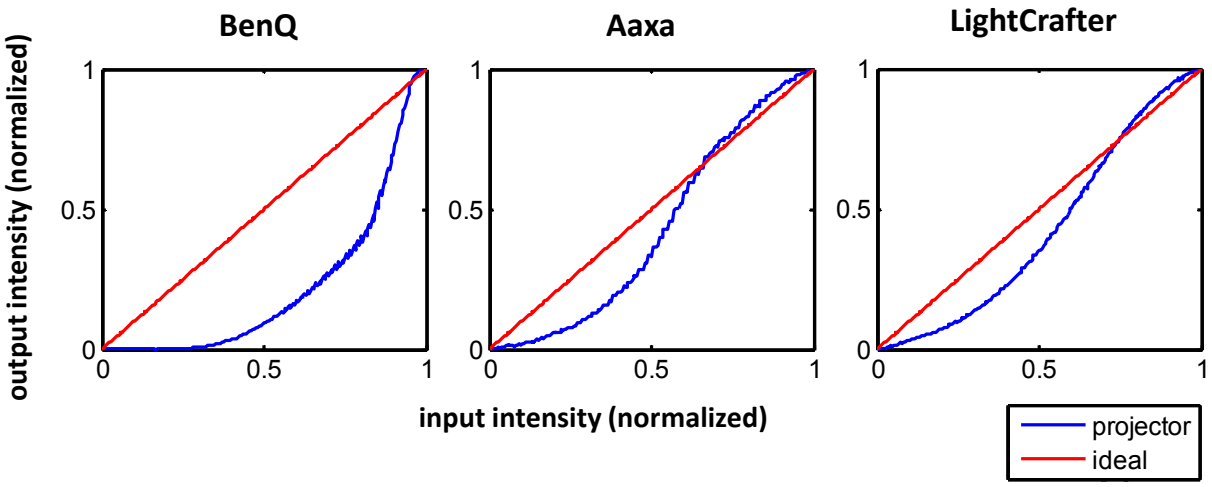

Figure 5 – Grayscale input/output curves for various COTS projection units including a BenQ PB8260 (left), an Aaxa M2 (middle), and a Texas Instruments LightCrafter (right)

After applying grayscale correction (described in the previous section) to the LightCrafter, the grayscale intensity curve became linear. As a result, the demodulated images we obtained were far better in quality when compared to those obtained without grayscale correction, as will be seen in **Figure 6**. The non-linearity in the initial grayscale output versus input curve is reflected in the detected sinusoidal pattern. It should be noted that this data was taken from a 99% Spectralon reflectance standard at a spatial frequency of 0.05 mm^{-1}, which is a common spatial frequency that we use to make SFDI measurements.

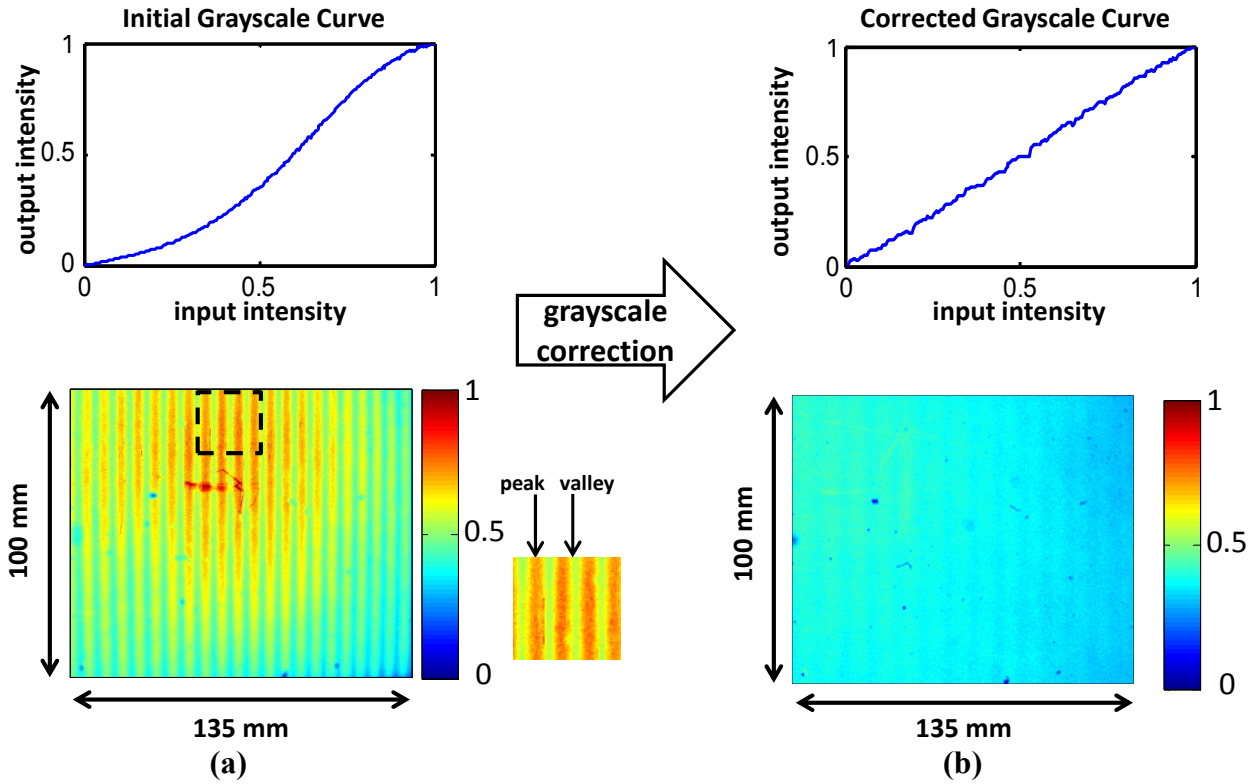

Figure 6 – (Top to Bottom) Grayscale calibration curves, and demodulated images before grayscale correction, showing artifacts (a), and after grayscale correction (b)

Spectral throughput data for the LightCrafter light engine is shown in **Figure 7**. Data is shown only for the LightCrafter because it is suitable for a handheld system, and is therefore applicable to this study. The ratio of output to input as a function of wavelength is given in **Figure 7**, which shows a clear degradation in output intensity beginning at around 700 nm, and decaying rapidly up to 900 nm, where there is virtually no signal. The ramifications of this degradation in the NIR region are significant, and will be discussed in Section 4.

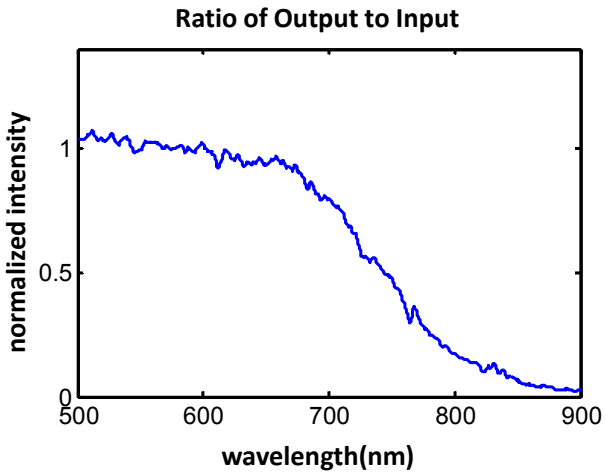

Figure 7 – Plots showing the ratio of the measured input spectrum to the measure output.

3.2 Light Sources

The temporal spectral stability data acquired from the LED modules is shown in **Figure 8**. For the LightCrafter LEDs, we measured peak wavelengths at 470, 535, and 625 nm, which correspond to the peak wavelengths of the blue, green, and red LEDs respectively. For the Roithner 970 nm module, we measured a peak wavelength at 970 nm, as expected.

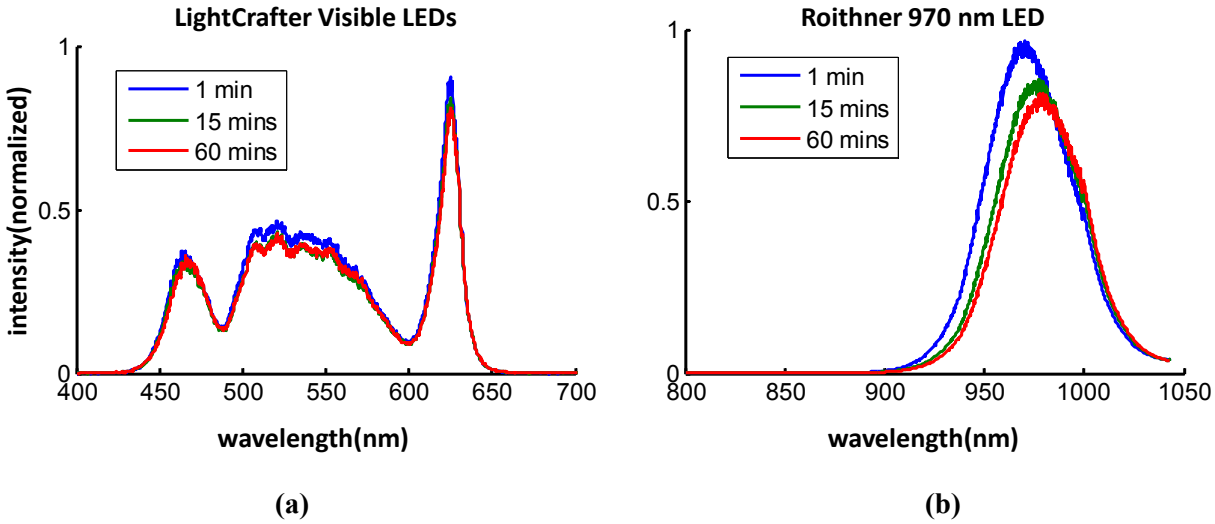

Figure 8 – Plot of LightCrafter visible (a) and Roithner Lasertechnik NIR (b) LED spectra as a function of time

Over the course of an hour, we observed an overall reduction in measured intensity of about 10% for the visible LEDs, and 15% for the NIR LED. Over that same period of time, we see minimal shifting of the peak wavelength for the visible LEDs, and a red-shifting of approximately 10 nm for the NIR LED. These changes occurred predominantly within the first 15 minutes after powering up. The decrease in amplitude and wavelength shifting were a consequence of the heating of the LEDs. One way to account for these effects in an SFDI system is to use thermo-electric cooling (TEC) [13]. However, implementation of TEC in a handheld system is not ideal, as it can add to the form factor of the final device. We will discuss possible alternatives to TEC in Section 4.

We also investigated the effect of increasing current to the LED. These results are shown in **Figure 9**. We observed that as input current is increased, the output intensity increased. However, the spectrum was also red-shifted as a function of input current. As input currents were increased in increments of one ampere, the amount of heat generated by the component was greater, so the shifting was also likely due to heating.

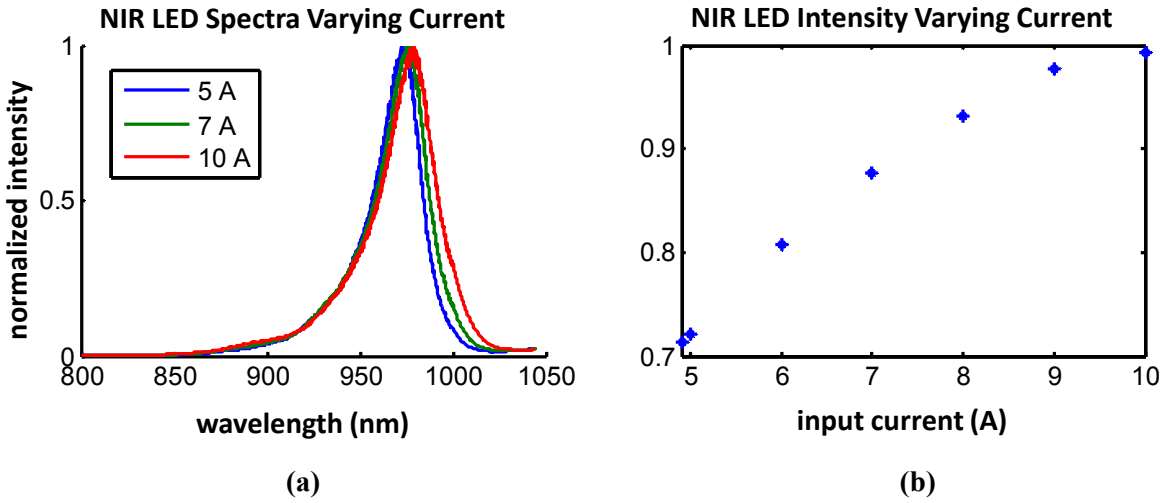

Figure 9 – Normalized spectra (a) and intensity at peak wavelength (b) of Roithner Lasertechnik (NIR) LED module

3.3 Camera

Similar to the projector throughput experiment, we also analyzed the throughput of two camera lenses (Schneider Kreuznach and Panasonic Lumix). This data is depicted in **Figure 10**a. We show that the throughput of the research-grade (Kreuznach) lens is excellent for all wavelengths tested, and that the consumer-grade (Lumix) lens throughput degrades in the NIR region, presumably a consequence of a manufacturer coating.

In **Figure 10b**, we show a plot of CCD throughput versus wavelength. The metric that we use to quantify throughput is relative efficiency, which is related to the number of photons converted to electrons, which are used to determine intensity. **Figure 10b** shows a significant degradation in relative efficiency in the NIR region, resulting in a greater than five-fold decrease from 500 nm to 900 nm.

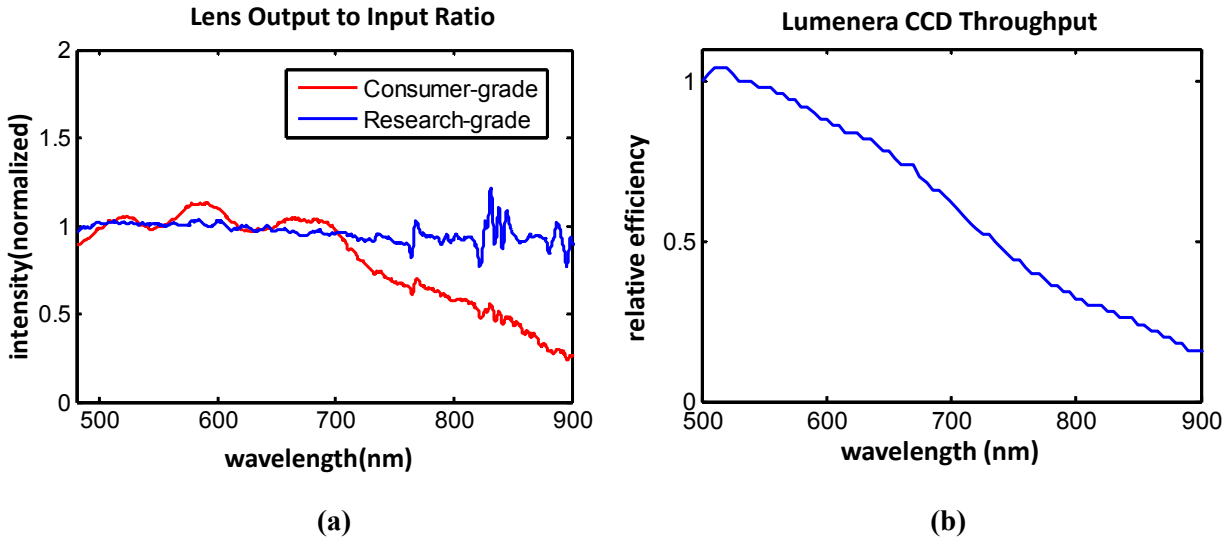

Figure 10 – Plots of consumer and research-grade lenses (a), and CCD (b) throughput

4. DISCUSSION

We have obtained several data sets relating to the performance of low cost, compact components to be integrated into a point-of care SFDI system. These datasets have helped identify a series of tests that are needed to evaluate any component before integration into an SFDI system. The primary properties that we test focus on grayscale calibration, spectral stability, and throughput. A list of these components, tests, and corresponding design requirements are shown in **Table 1**. This information and a set of performance tests will be critical to designing a robust, handheld SFDI imaging system.

Component	Test	Design requirement	Concern
Projector	1. Perform grayscale calibration 2. Test spectral throughput	1. Linear output 2. High NIR throughput	1. Output is not linear 2. Anti-NIR coatings
Light Source	1. Evaluate spectral stability 2. Evaluate spectral shifting 3. Evaluate spectral output vs. current	1. Minimize temporal change in spectrum 2. Minimize red-shifting due to heating 3. Proportional increase over all wavelengths	1. LED's have intrinsic warm-up times 2. LED thermal changes effect properties 3. LED properties change with current
Camera Lens	1. Test spectral throughput	1. High NIR throughput	1. Commercial Lens have anti NIR coatings
CCD	1. Test spectral throughput	1. High NIR throughput	1. CCD chips have intrinsic NIR deficiency

Table 1 – Summary of suggested tests to run for each hardware component with corresponding design requirements

In Section 3.1, we presented results pertaining to the grayscale intensity curves of COTS projectors. The data obtained using SFDI relies heavily on the precise spatial modulation of light. That is, the sinusoidal intensity patterns applied to the sample must be actual sinusoids. Therefore, it is critical that the SLM in an SFDI device produces accurate sinusoidal patterns. In COTS projection units, the grayscale output curve is often non-linear in order to account for the non-linear visual response curve of the human eye. This non-linearity makes sense for the purpose of video projection, but results in SFDI data with distinct artifacts. The grayscale calibration method proposed has shown to be a viable option to overcome this effect.

Another area of emphasis in this study has been the requirement to interrogate samples at specific wavelengths. This is directly related to the results obtained in Section 3.2, which highlights the spectral stability of visible and NIR LED modules. We found here that attenuation and spectral shifting over time were prevalent. We also showed that spectral shifting was present as we increased input current. In each case, we hypothesize that this shifting is due to heating of the LEDs, to which TEC was not applied due to size constraints. A barrier to developing a handheld device will be addressing these thermal issues. In order to account for temporal shifting, one possible solution may be to integrate a "standby" modality in order to allow the LEDs to warm up. We found that most of the shifting occurred during the first 15 minutes after power up, so another solution could be to simply wait for 15 minutes before using the device. This may be cumbersome, however, as a point-of-care device should have properties that allow for on-the-fly availability.

In Sections 3.1 and 3.3, we showed the limited spectral throughput for various components. Spectral throughput of components in the light path is directly related to the integrity of the obtained reflectance data and is ultimately used to compute chromophore concentrations. This will become even more relevant when cross polarization, which is used to suppress specular reflection from the sample surface, is integrated into the system. For rough surfaces such as skin, cross polarization is necessary for subsurface interrogation [8]. Since throughput in the NIR region is essential to calculating the concentration of many chromophores (i.e. oxy/deoxy-hemoglobin, water, etc.), we will eventually need to address the lack of NIR throughput issue prevalent in projectors, lenses, and detectors. One option may be to simply find other components whose internal optics do not reject NIR signals. Another option could be to remove the anti-IR coating on the internal optics, or replace these internal components with uncoated components.

In order to evaluate the performance of our device, we must run tests on phantoms with known optical properties that closely mimic human skin. We have already devised a method for fabricating such phantoms [14]. In future studies, these phantoms will be used to evaluate the performance of our system in the context of a clinical scenario.

3. CONCLUSION

We have analyzed several compact and low cost hardware components, and have presented data relevant to the component evaluation for implementation of a handheld point-of-care SFDI device. We have investigated system characteristics including grayscale linearity, spectral stability, and throughput, and related them to how they affect SFDI meaasurements. Although we will use this information to develop a specific device, one can apply the same experimental framework to develop most if not all SFDI devices.

ACKNOWLEDGMENTS

The authors gratefully acknowledge funding provided by the NIH NIBIB Biomedical Technology Research Center LAMMP: P41EB015890, NIH NIBIB 1R03EB012194-01, NIH SBIR R43RR030696, the Military Photomedicine Program, AFOSR Grant No. FA9550-08-1-0384, and the Beckman Foundation. Kyle P. Nadeau was partially supported by the NSF IGERT Biophotonics across Energy, Space, and Time fellowship.

REFERENCES

1. Gregory M.G., Vogel J.E., Kolk C.V., "Standardizing Digital Photography: It's Not All in the Eye of the Beholder″. Plastic and Reconstructive Surgery, 2001. **108**(5).
2. Goldman R.J., "More than One Way to Measure a Wound: An Overview of Tools and Techniques. Advances in Skin & Wound Care", Skin and Wound Care, 2002. **15**(5).
3. Vestergaard M.E., Macaskill P., Holt P.E., Menzies S.W., "Dermoscopy compared with naked eye examination for the diagnosis of primary melanoma: a meta-analysis of studies performed in a clinical setting. " The British journal of dermatology, 2008. **159**(3).
4. Mazhar A., Sharif A.S., Cuccia D.J., Nelson S.J., Kelly K.M., Durkin A.J., "Spatial frequency domain imaging of port wine stain biochemical composition in response to laser therapy: A pilot study." Lasers in Surgery and Medicine, 2012. **44**(8).
5. Ayers F.R., Cuccia D.J., Kelly K.M., Durkin A.J., "Wide-field spatial mapping of in vivo tattoo skin optical properties using modulated imaging.", Lasers Surg Med, 2009. **41**(6).
6. Kaiser M., Yafi A., Cinat M., Choi B., Durkin A.J., "Noninvasive assessment of burn wound severity using optical technology: A review of current and future modalities." Burns, 2011. **37**(3).
7. Yafi A., Vetter T.S., Scholz T., Patel S., Saager R.B., Cuccia D.J., Evans G.R., Durkin A.J., "Postoperative Quantitative Assessment of Reconstructive Tissue Status in Cutaneous Flap Model using Spatial Frequency Domain Imaging.", Plastic and Reconstructive Surgery, 2011. **127**(1).
8. Cuccia D.J., Bevilacqua F.., Durkin A.J., Ayers F.R., Tromberg B.J., "Quantitation and mapping of tissue optical properties using modulated imaging. Journal of Biomedical Optics", 2009. **14**(2).
9. Cuccia D.J., Bevilacqua F., Durkin A.J., Tromberg B.J., "Modulated imaging: quantitative analysis and tomography of turbid media in the spatial frequency domain." Optics Letters, 2005. **30**(11).
10. Neil M.A.A., Juskaitis R., and Wilson T., "Method of obtaining optical sectioning by using structured light in a conventional microscope." Opt Lett, 1997. **22**(24).
11. Mazhar A., Dell S., Cuccia D.J., Gioux S., Durkin A.J., Frangioni J.V., Tromberg B.J., "Wavelength optimization for rapid chromophore mapping using spatial frequency domain imaging." Journal of Biomedical Optics, 2010. **15**(6).
12. Nguyen J.Q., Saager R.B., Cuccia D.J., Kelly K.M., Jakowatz J., Hsiang D., Durkin A.J., "Effects of motion on optical properties in the spatial frequency domain." Journal of Biomedical Optics, 2011. **16**(12).
13. Mazhar A., Sharif A.S., Saggese S., Choi B., Cuccia D.J., Durkin A.J. "Implementation of an LED-based clinical spatial frequency domain imaging system", Photonics West 2012. San Francisco, CA: SPIE.
14. Saager R.B., Kondru C., Au K., Sry K., Ayers F.R., Durkin A.J. "Multi-layer silicone phantoms for the evaluation of quantitative optical techniques in skin imaging", Photonics West. 2010. San Francisco, CA: SPIE.